LFA-1 Is Sufficient in Mediating Neutrophil Emigration in Mac-1–deficient Mice

Huifang Lu,* C. Wayne Smith,* Jerry Perrard,‡ Dan Bullard,§ LiPing Tang,‖ Scott B. Shappell,¶ Mark L. Entman,‡ Arthur L. Beaudet,§** and Christie M. Ballantyne*‡

*Speros P. Martel Laboratory of Leukocyte Biology, Department of Pediatrics, ‡Department of Medicine, §Department of Molecular and Human Genetics, ‖Section of Neonatology, Department of Pediatrics, ¶Department of Pathology, Baylor College of Medicine, and **Howard Hughes Medical Institute, Houston, Texas 77030

Abstract

To better define the specific function of Mac-1 (CD11b) versus LFA-1 (CD11a) and the other CD11 integrins in vivo, we have disrupted murine *CD11b* by targeted homologous recombination in embryonic stem cells and generated mice which are homozygous for a mutation in *CD11b*. A null mutation was confirmed by Southern blotting, RNase protection assay, immunohistochemistry, and flow cytometry. Neutrophils isolated from mice deficient in Mac-1 were defective in adherence to keyhole limpet hemocyanin–coated glass, iC3b-mediated phagocytosis, and homotypic aggregation. When challenged by thioglycollate intraperitoneally, Mac-1–deficient mice had similar levels of neutrophil accumulation in the peritoneal cavity at 1, 2, and 4 h. Treatment with mAb to LFA-1 blocked 78% of neutrophil accumulation in Mac-1–deficient mice and 58% in wild-type mice. Neutrophil emigration into the peritoneal cavity 16 h after the implantation of fibrinogen-coated disks was not reduced in Mac-1–deficient mice whereas neutrophil adhesion to the fibrinogen-coated disks was reduced by > 90%. Neutrophils from Mac-1–deficient mice also showed reduced degranulation. Our results demonstrate that Mac-1 plays a critical role in mediating binding of neutrophils to fibrinogen and neutrophil degranulation, but is not necessary for effective neutrophil emigration, which is more dependent upon LFA-1. (*J. Clin. Invest.* 1997. 99:1340–1350.) Key words: inflammation • integrins • cell adhesion molecules • fibrinogen • cell degranulation

Introduction

Patients with genetic deficiency of CD18, the common β_2 chain of the leukocyte integrins, have leukocyte adhesion deficiency type I (LAD I)[1] and profoundly reduced emigration of neutro-phils at sites of inflammation (1). This leads to a partial or total deficiency of the CD11/CD18 integrins from the cell surface which include CD11a/CD18 (LFA-1, α_{L2}), CD11b/CD18 (Mac-1, CR3, α_{M2}), CD11c/CD18 (P150,95, α_{x2}), and CD11d/CD18 (α_{d2}) (2–6). Although the genetic disorder LAD I has given great insight into the functional significance of the CD18 family, the relative contributions of each of the CD11 integrins in the phenotypic abnormalities seen in LAD I remain unclear. Early studies in mice using mAbs against CD11b led to the conclusion that CD11b/CD18 (Mac-1, CR3) is the dominant member of the CD18 family on neutrophils accounting for emigration (7, 8). This integrin is far more abundant in neutrophils than CD11a/CD18 (LFA-1) or CD11c/CD18 (p150,95), being contained in secretory granules that allow transport of Mac-1 to the cell surface after chemotactic stimulation (9). The intracellular pool appears to support sustained neutrophil locomotion on surfaces where adhesion is dependent on Mac-1 (10). However, a dominant role for Mac-1 in emigration has come into question as a result of more recent studies both in vitro and in vivo. Work from Issekutz et al. (11), Rutter et al. (12), and Graf et al. (13) in rat and rabbit models of inflammation have provided evidence that LFA-1 plays a dominant role in neutrophil emigration. Tang et al., in a mouse model of peritoneal inflammation (14), found that neutrophil inhibitory factor, a product from canine hook worms that inhibits Mac-1 but not LFA-1 adhesion (15), failed to reduce neutrophil emigration. These observations coupled with studies in vitro showing that anti-CD11b mAbs are consistently less effective in blocking transendothelial migration of neutrophils than anti-CD11a mAbs (16, 17) cast doubt on the earlier assumption that Mac-1 is the major determinant of neutrophil extravasation.

To better define the function of CD11b versus CD11a and the other CD11 integrins in vivo, we have disrupted the murine gene for *CD11b* by targeted homologous recombination in embryonic stem (ES) cells and generated a line of mice which are homozygous for the targeted mutation in *CD11b* (Mac-1 −/−). In this report, we assess distinctions between the functions of LFA-1 and Mac-1 in regards to neutrophil adhesion and extravasation in mice shown to be totally deficient in Mac-1.

Methods

Targeting construct and generation of mutant mice. A 245-bp CD11b cDNA fragment containing exons 2, 3, and 4 of murine CD11b was generated by reverse transcription (RT)-PCR of endotoxin-stimulated 129/Sv mouse spleen total RNA using synthetic primers derived from the published cDNA sequence (18) (5′-ATGGCTTCA-ATCTGGACAC-3′ and 5′-AGAAACAGCCAGGGACAGG-3′). The PCR product was subcloned, sequenced, and then used as a probe to isolate a genomic clone from a 129/Sv mouse library (Stratagene, La Jolla, CA). The genomic clone was characterized by restriction mapping, Southern blot analysis, and DNA sequencing. Two

1. *Abbreviations used in this paper:* ES, embryonic stem; KLH, keyhole limpet hemocyanin; LAD I, leukocyte adhesion deficiency type I; MPO, myeloperoxide; PET, polyethylene terephthalate; ZAS, zymosan-activated serum.

adjacent genomic restriction fragments of 6.3 and 5.3 kb containing exons 3–6 were ligated into the polylinker of pBluescript SK$^+$ (Stratagene). A neomycin cassette driven by the mouse RNA polymerase II promoter was inserted between a HindIII site and an XhoI site within the 5.3-kb fragment. This insertion results in replacement of 700 bp of the *CD11b* gene which contains exon 4, leaving 2.3 kb of 5′ genomic DNA and 8.6 kb of 3′ genomic DNA flanking either side of the neomycin cassette (Fig. 1). The vector was linearized in the polylinker on the 3′ side with digestion by SalI.

The AB2.1 ES cell line (provided by Allan Bradley, Baylor College of Medicine) was electroporated with 25 μg/ml of linearized vector as described (19). After selection with G418, individual colonies were picked and screened for targeted homologous recombination by Southern blotting using a microextraction procedure (20) with a 400-bp probe developed from 5′ flanking DNA that was not in the construct as indicated in Fig. 1. Cells confirmed by Southern blotting to carry the replacement mutation were injected into day 3.5 C57BL/6J blastocysts and transferred into foster mothers. Chimeric males were mated with C57BL/6J females, and germline transmission was confirmed by Southern blotting of tail DNA after digestion with EcoRI.

RT-PCR. Total RNA was isolated by the guanidinium isothiocyanate phenol extraction method from bone marrow and spleen tissues from mice which were homozygous for the targeted mutation in CD11b (−/−) and wild-type littermates (+/+) 3 h after intraperitoneal injection with 50 μg of lipopolysaccharide (Difco Laboratories Inc., Detroit, MI). First strand complementary DNA was synthesized from equal quantities of total RNA using poly dT oligo and AMV reverse transcriptase. Primer pairs used for PCR included: exons 3–6 (5′-AGGAGGCAAAGGCTGTTAAC-3′ + 5′-TGTTGTTGATGC-TACCGGAG-3′). PCR consisted of 5% of the total cDNA, 50 pmol of each primer, 0.2 mM each dNTP, 10 mM Tris-HCl, 50 mM KCl, 1.5 mM magnesium chloride, and 2.5 U *Taq* DNA polymerase (Pro-

mega, Madison, WI) in a 50-μl reaction volume. Cycling parameters were 94°C for 5 min followed by 35 cycles of 94°C for 1 min, 55°C for 1 min, and 72°C for 2 min.

RNase protection assay. A PCR product spanning from exon 3 to exon 6 (see above) was subcloned in PCRII vector (Invitrogen Corp., San Diego, CA). The insert orientation was determined by DNA sequencing and the vector was linearized at the 5′ end of the insert in the polylinker. Antisense ^{32}P-labeled transcripts were synthesized at 37°C in reaction containing 1 μg linearized template DNA, 1 mM each of ATP, GTP, and UTP, 70 μCi [α-^{32}P]CTP (400 Ci/mmol), 10 U T7 RNA polymerase, and standard transcription buffer. The probe was purified by two rounds of precipitation with ammonium acetate and ethanol. RNase protection was performed using the RNase protection kit (Boehringer Mannheim, Indianapolis, IN) according to the manufacturer's instructions. Briefly, 80 μg total RNA was hybridized with 300,000 CPM ^{32}P-labeled riboprobe overnight at 50°C followed by RNase digestion. An RNase protection assay using yeast tRNA as a target was performed to confirm that there was no self protection of the riboprobe.

The protected fragments were resolved on a 6% denaturing polyacrylamide gel followed by autoradiography for 24 h. Molecular weights of protection fragments were determined by comparison to the protection fragments from the synthetic sense transcript as well as DNA sequencing ladder (data not shown).

Flow cytometry analysis. Peripheral blood of anesthetized mice was collected from the retroorbital plexus in heparin-capillary tubes or by cardiac puncture at the time of death. 100 μl of whole blood was stained with antibodies: FITC anti-CD11b (M1/70), biotinylated anti-CD11a (KBA) followed by streptavidin PE, PE anti–Gr-1 (clone RB6-8C5; PharMingen, San Diego, CA), and anti-CD18 (C71/16) followed by FITC secondary antibodies. Cells stained with directly conjugated antibodies were incubated at room temperature for 15 min in
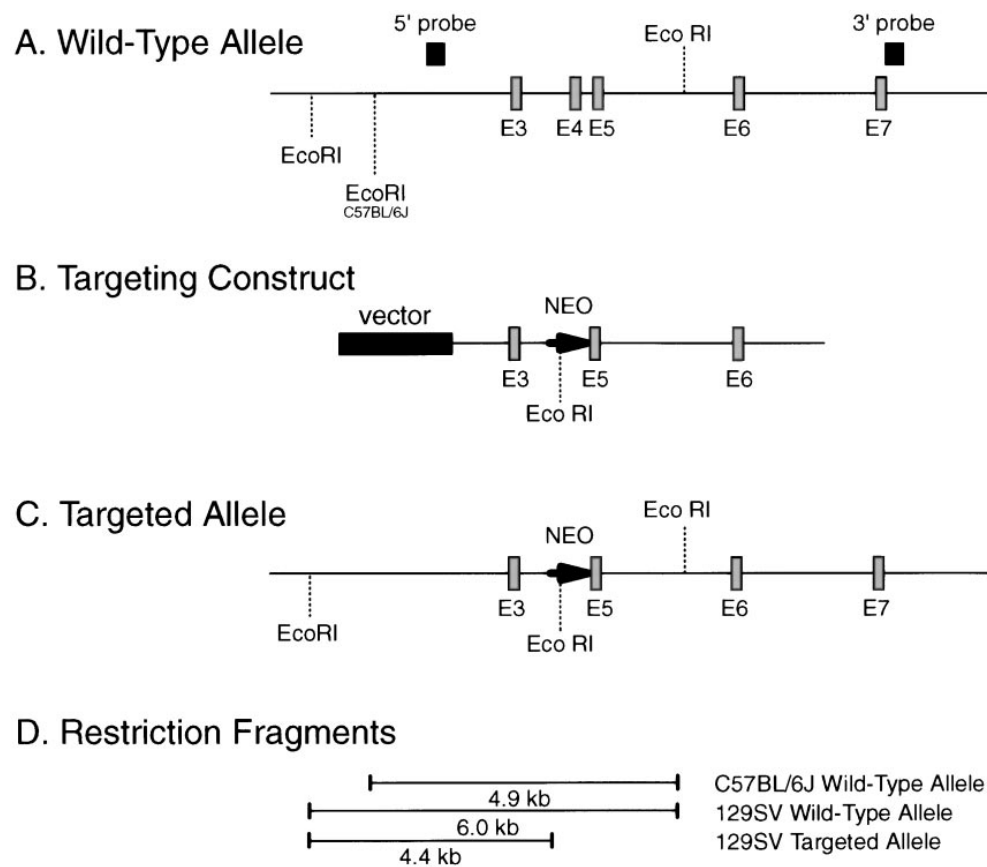

Figure 1. Targeting construct and homologous recombination. (*A*) Partial EcoRI restriction map of the murine *CD11b* gene. Boxes represent exons 3–7. The 5′ and 3′ probes were derived from flanking DNA not used in the construct. (*B*) The CD11b replacement construct results in the replacement of 700 bp of the CD11b gene that contain exon 4 with a neomycin resistance cassette (*NEO*) leaving 2.3 kb of 5′ genomic DNA and 8.6 kb of 3′ genomic DNA. (*C*) Map of the predicted homologous recombinant event. (*D*) EcoRI digest leads to a 4.4-kb fragment as compared with the 6.0-kb fragment in wild-type 129/Sv. The restriction fragment in wild-type allele for C57BL/6J is 4.9 kb.

the dark. Cells stained with anti-CD18 were washed three times and added with FITC goat anti–rat secondary antibody for 15 min. Cells were then fixed in 1% paraformaldehyde before analysis on FAC-Scan® (Becton-Dickinson, Mountain View, CA).

Immunohistochemistry. Frozen sections of major organs of CD11b mutant mice were stained using a modified avidin-biotin peroxidase technique, as described previously (21). 6-μm sections were fixed in cold acetone for 6 min, stored at −80°C, and prewarmed to room temperature for at least 2 h before use. Endogenous avidin binding activity was blocked by preincubation with avidin D followed by biotin solutions (Vector Laboratories, Burlingame, CA) according to the manufacturer's instructions. Sections were incubated with primary antibody M1/70 (anti-CD11b) at 5 μg/ml diluted in PBS with 1% BSA (GIBCO BRL, Gaithersburg, MD) at room temperature for 1 h and then incubated with biotinylated goat anti–rat (1:1,000; Caltag Laboratories, San Francisco, CA) secondary antibody diluted in PBS with 1% BSA at room temperature for 1 h. All sections were then incubated for 1 h with avidin–biotin complex (Vector Laboratories) and developed with a 10-min incubation in a 50 mg% solution of diaminobenzidine in Tris buffer (pH 7.5) activated with a 1:1,000 dilution of 30% H_2O_2. Sections were counterstained with methyl green-alcian blue, dehydrated, and mounted.

Isolation of neutrophils. After mice were killed by cervical dislocation under anesthesia, femurs and humeri were removed aseptically to obtain bone marrow. Murine neutrophils were partially isolated from mononuclear leukocytes by NIM.2 Hypaque-Ficoll density gradient centrifugation (Cardinal Associates, Santa Fe, NM). Isolated bone marrow neutrophils were of 70–75% purity as assessed by Neat stain (Midlantic Biomedical Inc., Paulsboro, NJ). Cells were washed and resuspended in PBS.

Adhesion assay. Keyhole limpet hemocyanin (KLH; Sigma Chemical Co., St. Louis, MO)–coated glass coverslips were used as Mac-1–specific substrate (22). A visual static adhesion assay of isolated neutrophils was performed as described in detail previously (23). In studies designed to evaluate the involvement of β_2 integrins in neutrophil adhesion to KLH-coated glass, cells were preincubated with mAbs at room temperature for 30 min: 10 μg/ml M1/70 (anti-CD11b), 10 μg/ml KBA (anti-CD11a), or 10 μg/ml SFDR5 (anti-HLA, Ig-matching control). Chemotactic stimulus for mouse neutrophils (1% zymosan-activated serum [ZAS]) was added immediately before injecting the cell mixture into the adhesion chamber.

Homotypic aggregation of neutrophils. Neutrophils isolated from mouse bone marrow were maintained in PBS (without Ca^{2+} and Mg^{2+}). Suspensions of neutrophils added to siliconized cuvettes containing a stir bar were allowed to warm to 37°C for 1 min with constant stirring at 700 rpm with and without mAbs in an aggregometer (model 300B; Payton Scientific Inc., Buffalo, NY). PBS containing 1.5 mM Ca^{2+} and Mg^{2+} was added coincidently with PMA or 10% ZAS. Cells were at a final concentration of 3×10^6 in a volume of 0.4 ml. 20-μl aliquots of cell suspension were fixed in 100 μl of 2% glutaraldehyde in PBS at 0, 0.5, 1, 3. 5, 10, and 15 min. Cells were allowed to fix for a minimum of 30 min before being analyzed on a FACScan® flow cytometer (Becton Dickinson) using a sampling flow rate of 60 μl/min. 4,000 events per sample were collected and the determination of singlet (S) neutrophils could be discriminated from doublets (D) or higher aggregates [triplets (T), quadruplets (Q), and pentruplets (P)] by analysis of the autofluorescence histogram (FL2 emission at 564–606) as described by Rochon et al. (24). Percent aggregation was calculated as frequency of singlets recruitment: *% aggregation = Fs = S ÷ [S + 2*(D) + 3*(T) + 4*(Q) + 5*(P)]*.

Assays of luminol-enhanced chemiluminescence. The evolution of light from neutrophils undergoing iC3b-mediated phagocytosis after activation by opsonized zymosan particles was quantitated as described previously (25). Zymosan particles (ICN Pharmaceuticals, Cleveland, OH) were opsonized in freshly obtained serum from healthy mice for 45 min at 37°C. Opsonized zymosan particles were then washed three times and resuspended in PBS to a final concentration of 0.5 mg/ml. Phagocytotic reaction mixtures contained 10^6 neu-

trophils with 10^{-8} M luminol. Chemiluminescence was quantitated after the addition of PBS, 10 ng/ml PMA, or 0.5 μg/ml of opsonized zymosan particles to reaction mixture.

Homotypic aggregation of T lymphocytes. T lymphocytes were isolated from spleen of wild-type and CD11b-deficient mice according to standard procedure (26). Cells were resuspended in DMEM, 10% FCS, glutamine (200 mM), and B-mercaptoethanol (10^{-6} M). Subsequently, $2.5–4 \times 10^5$ cells per well (200 μl) were added to 96-well plates and incubated for 24 h in the presence of PBS or 1 ng/ml PMA plus 200 ng/ml Ionomycin (Sigma Chemical Co.). Aggregation was observed and determined as either present or absent using light microscopy.

Thioglycollate-induced peritonitis. Wild-type and CD11b-deficient mice as littermates were injected intraperitoneally with 1 ml 2.4% thioglycollate or 1 ml PBS at time 0. At +1, +2, and +4 h mice were injected intraperitoneally with 3 ml of ice-cold PBS (without Ca^{2+}, Mg^{2+}, with 50 U/ml heparin), their abdomens were massaged, and total lavage fluid was withdrawn. Total cell number was determined by Coulter Counter (Coulter Electronics Ltd., Luton, United Kingdom). Peritoneal cell pellet was resuspended, and differential counts were performed after cytospin and Neat stain. Neutrophil number was determined by multiplying the total cell number times the percentage of neutrophils on the differential count. In experiments assessing the contribution of CD11a or CD11b, animals were injected with appropriate mAbs. KBA (anti-CD11a), M1/70 (anti-CD11b), or SFDR5 (nonbinding isotype-matched mAb) was injected intraperitoneally (6 mg/kg) at −16 h and intravenously (9 mg/kg) at −1 h. F(ab')₂ fragments of the antibodies were made using the Immunoaffinity Pak kit (Pierce Chemical Co., Rockford, IL).
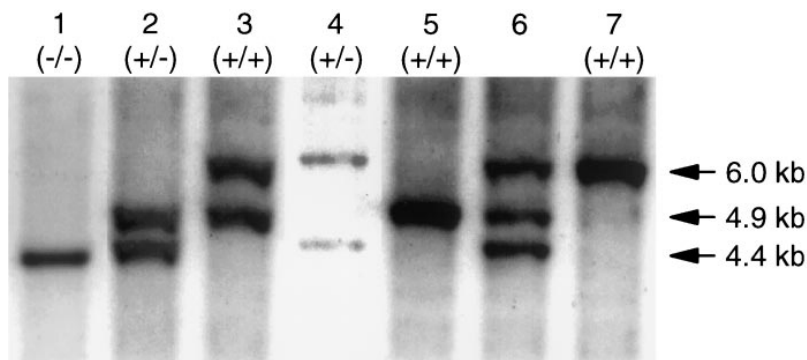
Assessment of Mac-1–dependent adhesion in vivo. Fibrinogen-coated polyethylene terephthalate (PET) (Mylar) disks (type a, 0.005 mm thick; Cadilla Plastic and Chemical Co., Birmingham, MI) of 1.2 cm in diameter were prepared as described previously (27). Three disks were then implanted intraperitoneally in each age-matched wild-type mouse and CD11b-deficient mouse. Peritoneal lavage using 5 ml of warm PBS was performed 16 h later and PET disks were removed at the same time. Total cell count and differentials in the lavage were determined. Myeloperoxide (MPO) activity of the total cell pellet from the peritoneal lavage and cells adherent to the disks was determined separately as described previously (14). MPO levels were determined per neutrophil and the data expressed as numbers of neutrophils in the lavage fluid or on the disks.

β-glucuronidase assay. β-glucuronidase from peripheral and peritoneal neutrophils was assayed as described previously (28). Peripheral blood from four wild-type and CD11b-deficient mice was collected to isolate neutrophils. Wild-type or homozygous mutant (−/−) littermates were injected intraperitoneally with 1 ml of thioglycollate medium. 4 h after injection, 3 ml of ice-cold PBS with 50 U/ml of heparin was injected intraperitoneally and peritoneal lavage fluid was withdrawn. After the total neutrophil count was determined, the cell pellet was lysed in 0.2% Tween 20. An aliquot of lysate equivalent to 10^6 cells was added to 100 μl of 5 mg/ml phenolphthalein glucuronic acid, pH 4.6, and incubated at 37°C overnight. Reactions were stopped 16 h later by adding 1 ml of glycine (pH 10.2). Samples were then measured by spectrophotometer at 540 nm. Peritoneal neutrophil β-glucuronidase activity was divided by that of the peripheral activity and multiplied by 100 to provide a percentage of the enzyme retained after the transmigration.

Statistics. Statistical comparisons were made by Student's *t* test or ANOVA and Dunnett's test for multiple comparisons to control means.

Results

Generation of mice deficient in CD11b and molecular characterization. ES cells with a targeted event had a 4.4-kb EcoRI fragment identified by the 5′ flanking probe on Southern blot compared with the 6.0-kb fragment in wild-type 129/Sv mice

Figure 2. Genotype analysis of DNA from mouse tails and ES cells by Southern blot analysis with a 5′ flanking probe. CD11b genotype is indicated above each lane: (+) for wild-type allele and (−) for targeted allele. The mutant, C57BL/6J wild-type, and 129/Sv wild-type alleles are identified by 4.4, 4.9, and 6.0 kb EcoRI fragments, respectively. Differences in size between the 129/Sv and C57BL/6J wild-type fragments are due to a restriction fragment length variation. All three alleles are present in tail DNA from chimeric mice, but only the 129/Sv wild-type or mutant alleles are transmitted in the germline. (Lane *1*) DNA from a mouse homozygous for the targeted mutation, (lane *2*) heterozygous mouse, (lane *3*) wild-type mouse with C57BL/6J allele identified by the 4.9-kb EcoRI fragment and the 129/Sv allele identified by the 6.0-kb EcoRI fragment, (lane *4*) the ES cell clone used for injections, (lane *5*) wild-type C57BL/6J, (lane *6*) chimera, and (lane *7*) wild-type 129/Sv.

(Fig. 1). Targeted ES cell clones were injected into C57BL/6J blastocysts and male chimeric offspring that were > 90% agouti coat color were bred to C57BL/6J mice. Germline transmission was confirmed by Southern blotting studies. The expected targeted allele of 4.4 kb was identified by the 5′ flanking probe on Southern blots of mice heterozygous for the mutation (Fig. 2). The wild-type restriction fragment of 6.0 kb was observed in offspring that did not inherit the targeted allele (Fig. 2). Wild-type C57BL/6J mice have an EcoRI restriction fragment of 4.9 kb identified by the 5′ probe due to a genetic strain variation. Thus the wild-type C57BL/6J, wild-type 129/Sv, and mutant 129/Sv alleles are identified by EcoRI restriction fragments of 4.9, 6.0, and 4.4 kb, respectively. Confirmation of a replacement event was performed using a 3′ flanking probe which also showed the predicted change in restriction fragment pattern (data not shown). In addition, a probe derived from exon 4 was also used in Southern blots of DNA from mice homozygous for the mutation which confirm that exon 4 was deleted in the mutant mice but present in the wild-type mice (data not shown).

RT-PCR was performed on total RNA from bone marrow of wild-type and homozygous mutant mice using two pairs of oligos. PCR using a 5′ oligo in exon 3 and a 3′ oligo in exon 6 resulted in amplification of the predicted 347-bp fragment from wild-type RNA and a fainter 276-bp fragment from mutant RNA (data not shown). DNA sequence analysis revealed that the smaller fragment was identical to the 347-bp wild-type fragment with the exception that it lacked exon 4. Sequence analysis of the murine *CD11b* gene shows that splicing exon 3 to exon 5 leads to a frame shift mutation and a nonsense peptide. To confirm the PCR results, RNase protection analysis was performed on total RNA from spleen and bone marrow of wild-type and homozygous Mac-1(−/−) mice using a ^{32}P-labeled antisense riboprobe spanning from exon 3 to exon 6 in the murine CD11b mRNA. One major protected fragment was observed with RNA from wild-type mice, but not with RNA from Mac-1(−/−) mice, corresponding to the full-length mRNA with a predicted size of 347 nt (Fig. 3). A protected fragment of 95 nt corresponding to exon 3 and a fragment of 181 nt corresponding to exons 5 and 6 were observed with RNA from Mac-1(−/−) mice. These results are consistent with the presence of an alternatively spliced RNA lacking exon 4. The higher intensity of the 95 nt fragment indicated that most transcripts in the mutant terminate in the neomycin cassette, whereas a much smaller number is alternatively spliced. An RNase protection assay using yeast tRNA as a control yielded no protected fragments. All protected fragments were of higher intensity in bone marrow RNA, indicating a higher mRNA level of murine CD11b in bone marrow than in spleen.

Homozygous and heterozygous mutant mice were born in expected ratio and were fertile. Mutant mice did not demon-
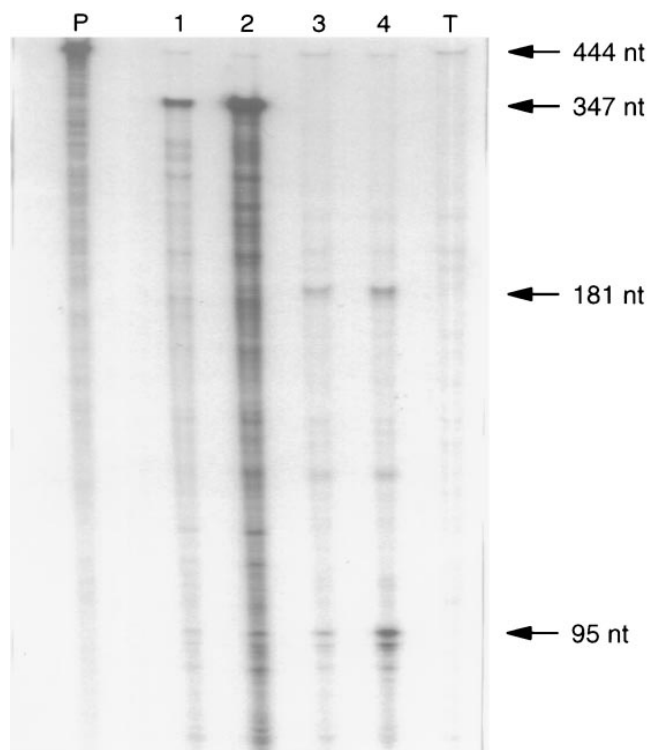

Figure 3. RNase protection analysis. Analysis was performed as described in Methods. Probe (*P*), wild-type spleen RNA (lane *1*), wild-type bone RNA (lane *2*), mutant spleen RNA (lane *3*), mutant bone RNA (lane *4*), and yeast tRNA (*T*). The probe contains 97 nt of vector DNA that is unprotected by the CD11b transcript. The 347-nt fragment corresponds to the full-length wild-type transcript. The 95-nt and 181-nt protected fragments correspond to exon 3 and exons 5 and 6, respectively.
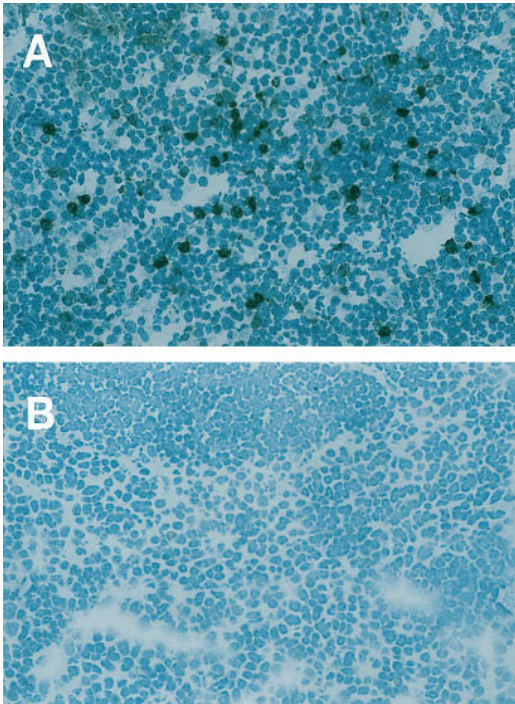
Figure 4. Immunohistochemistry of spleen from wild-type and CD11b-deficient mice. Wild-type (*A*) and CD11b-deficient mice (*B*) were killed 6 h after intraperitoneal injection of lipopolysaccharide. Spleens were stained with the M1/70 monoclonal antibody to mouse CD11b. There is no detectable staining seen in mutant mouse. ×400.

strate any gross abnormalities in growth rate and tissue architecture of major organ systems. However, out of about 268 homozygous Mac-1–deficient mice we have bred, 3 have developed bacterial abscesses involving salivary glands. Bacterial cultures recovered *Proteus mirabilis* and *Staphylococcus aureus*. Such abscesses did not occur in wild-type littermates.

Immunocytology. Major organs of Mac-1–deficient mice were fixed and stained for CD11b expression. There was significant CD11b staining in the spleen of wild-type mice (Fig.

4 *A*), but no detectable CD11b staining in Mac-1–deficient (−/−) mice (Fig. 4 *B*). Deficiency of CD11b expression on neutrophils was confirmed by flow cytometric analysis of peripheral blood stained with specific mAbs. Anti-CD11b mAb M1/70 binds to Mac-1 on wild-type neutrophils, but there was no detectable CD11b staining on neutrophils from Mac-1–deficient mice (Fig. 5). CD11b on neutrophils from heterozygous mice (+/−) was also reduced compared with wild-type mice. CD18 expression on Mac-1−/− neutrophil was 60% of that on wild-type neutrophils. Surface expression of LFA-1 was not different on neutrophils from Mac-1–deficient (−/−) versus wild-type mice (Fig. 5).

In vitro studies of leukocyte adherence. Using glass coated with KLH as substrate for neutrophil adhesion in vitro (22), we documented that neutrophils from wild-type mice adhered to KLH when activated by 1% ZAS. Such adhesion was inhibited by mAb M1/70 (anti-CD11b) (Fig. 6 *A*), but not by KBA (anti–LFA-1) or the control mAb SFDR5 (data not shown). In the presence of 1% ZAS as stimulus, neutrophils from CD11b-deficient mice did not adhere to KLH-coated glass (Fig. 6 *A*). Neutrophils from mice which were heterozygous for the CD11b mutation exhibited normal adhesion to KLH-coated glass (data not shown).

Homotypic aggregation of neutrophils after stimulation with chemotactic factors has been found to be largely dependent on CD11b/CD18 (29). When stimulated with 10% ZAS, ∼ 40% of normal neutrophils were recruited into aggregates within 60 s (Fig. 6 *B*). With the same stimulation, ∼ 17% of CD11b-deficient neutrophils were recruited into aggregates by apparently CD11b-independent mechanisms since it could not be inhibited by anti-CD11b (M1/70) (data not shown).

The evolution of light by neutrophils undergoing iC3b-mediated phagocytosis was quantitated by a luminol-enhanced chemiluminescence assay (29). Neutrophils isolated from wild-type mice exhibited substantial chemiluminescence when mixed with opsonized zymosan particles. CD11b-deficient neutrophils did not release chemiluminescence when mixed with opsonized zymosan (Fig. 6 *C*). When stimulated with PMA, however, CD11b-deficient neutrophils exhibited similar chemiluminescence as wild-type neutrophils.
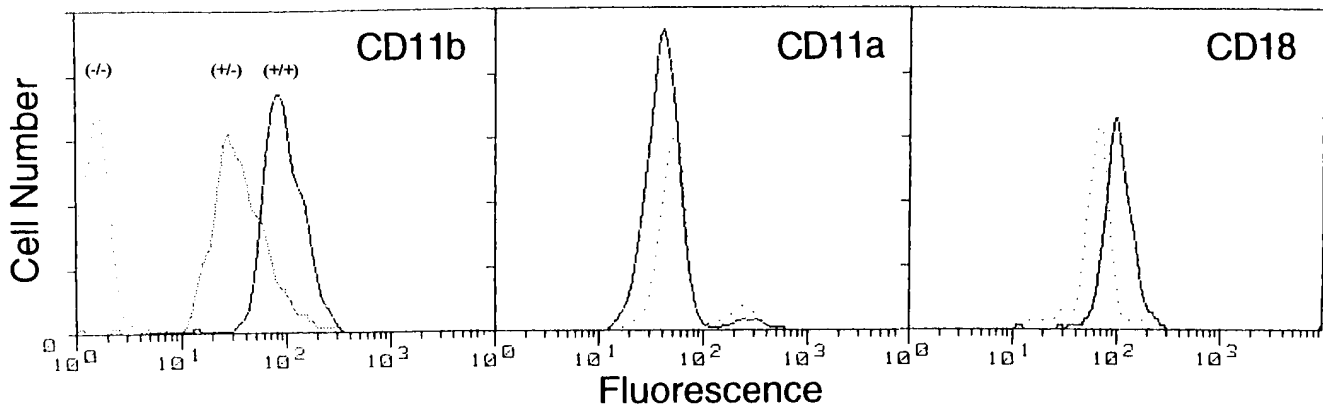

Figure 5. Expression of CD11b, CD11a, and CD18 on wild-type and CD11b mutant mice. Heparinized peripheral blood was incubated with FITC-labeled anti-CD11b (M1/70), biotinylated KBA (anti-CD11a), followed by streptavidin PE, or anti-CD18 (C71/16) followed by FITC-labeled secondary antibody for 15 min. Stained cells were analyzed on a FACScan® flow cytometer. Wild-type (+/+) mice are indicated by a solid line, homozygous (−/−) mice for the CD11b mutation are indicated by the spaced dotted line, and mice heterozygous (+/−) for the CD11b mutation are shown on the left by the stippled line.
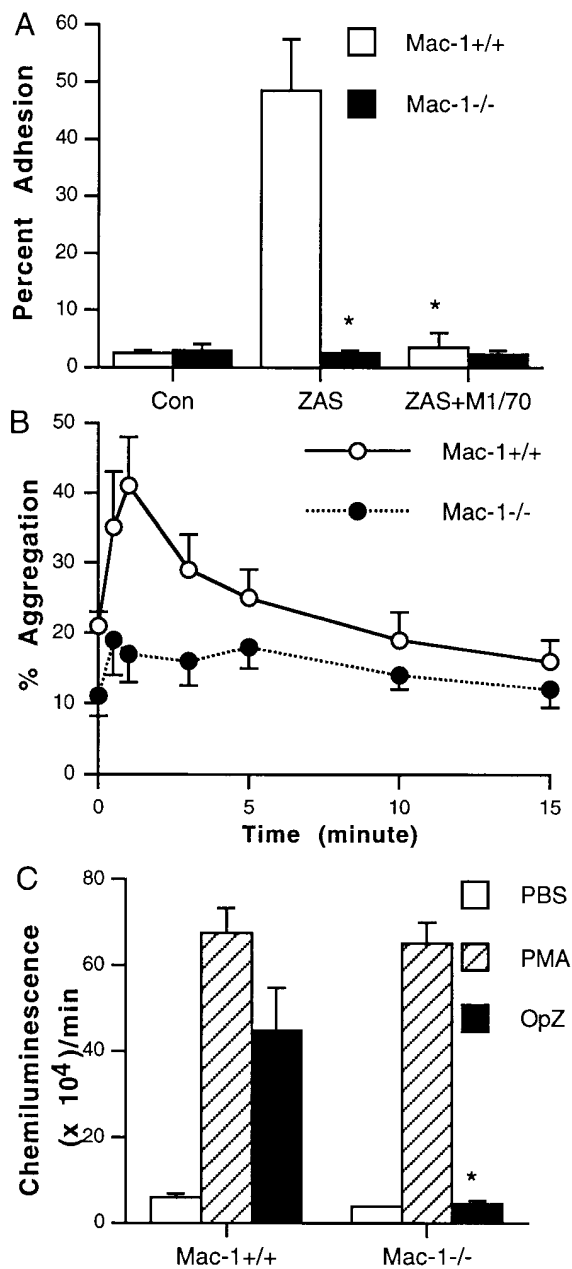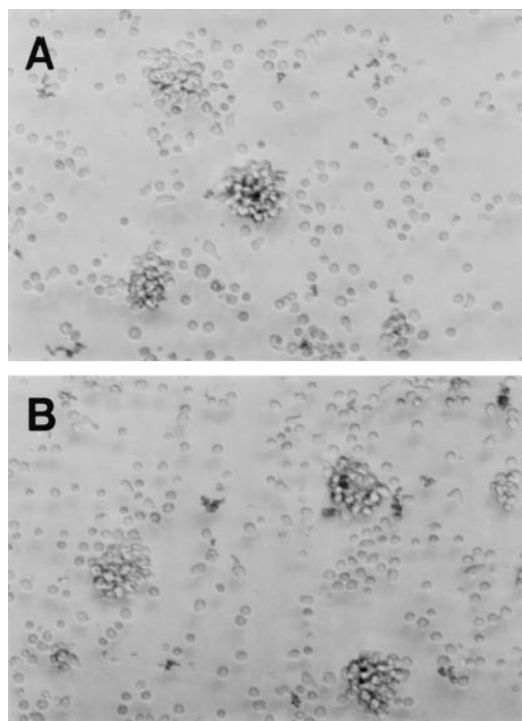
Figure 7. Homotypic aggregation of isolated T lymphocytes. Cells isolated from spleen were stimulated in culture for 16 h with 1 ng/ml of phorbol 12-myristate 13-acetate and 200 ng/ml of ionomycin. Aggregation of T lymphocytes was present in both wild-type (*A*) and mutant mice (*B*) observed by light microscopy.

Figure 6. In vitro adherence of neutrophils. (*A*) Adherence of isolated neutrophils to KLH-coated glass. Isolated neutrophils were incubated with PBS (*Con*) or mAb for 30 min at room temperature: 10 μg/ml M1/70 (anti-CD11b). ZAS was added immediately before injecting the cell mixture into the adhesion chamber. Neutrophil adherence was determined using a visual static assay at room temperature. $n = 4$. *$P < 0.01$. (*B*) Homotypic aggregation of isolated neutrophils in response to ZAS. Neutrophils suspended in Ca^{2+}-free PBS (3×10^6/ml) were added to siliconized cuvettes and allowed to warm to 37°C for 1 min. PBS containing 1.5 mM Ca^{2+} and Mg^{2+} was added coincidently with 10% ZAS. 20-μl aliquots of cell suspension were fixed in 100 μl of 2% glutaraldehyde in PBS at 0, 0.5, 1, 3, 5, 10, and 15 min. Cells were allowed to fix for a minimum of 30 min before being analyzed on a FACScan® flow cytometer. Percent of aggregation was calculated as frequency of singlet recruitment into aggregates. Empty circles represent wild-type mice and filled circles represent CD11b-deficient mice, $n = 3$. (*C*) Chemiluminescence of neutrophils from wild-type and CD11b-deficient mice. Isolated neutrophils were mixed with 10^{-8} M luminol before the addition of PBS, 10 ng/ml of PMA, or 0.5 μg/ml of freshly opsonized zymosan particles (*OpZ*). Result represents mean±SEM, $n = 4$, *$P < 0.01$.

Peripheral blood lymphocytes have been shown to aggregate in response to phorbol esters, and this adhesion can be blocked by anti–LFA-1 mAb. Lymphocyte aggregation stimulated in this fashion is dependent on LFA-1/ICAM-1 interactions (30). To assess this LFA-1–dependent function, we incubated murine T lymphocytes isolated from spleen cells with PMA for 16 h and monitored aggregation. LFA-dependent T cell homotypic aggregation occurred to the same extent in CD11b-deficient mice as in the wild-type mice (Fig. 7).

Kinetics of neutrophil influx in thioglycollate-induced peritonitis. After thioglycollate injection, peritoneal lavage was collected at 1, 2, and 4 h (Fig. 8 *A*). CD11b-deficient mice had similar levels of neutrophil accumulation in the peritoneal cavity at each time point (T = 1, 2, and 4 h) with no significant difference from wild-type controls. Neutrophil numbers were $1.56\pm0.65 \times 10^6$, $4.2\pm0.99 \times 10^6$, and $15.3\pm1.5 \times 10^6$ for wild-type mice and $3.17\pm1.3 \times 10^6$, $5.25\pm0.9 \times 10^6$, and $19.6\pm3.3 \times 10^6$ for CD11b-deficient mice.

To investigate the specific contribution of LFA-1 and Mac-1 to neutrophil emigration in this thioglycollate-induced peritonitis, mice were treated systemically with mAb KBA (anti–LFA-1) or a control antibody SFDR5. 4 h after thioglycollate injection, peritoneal lavage was collected. KBA caused a maximum of 78% inhibition of neutrophil accumulation in CD11b-deficient mice and 58% inhibition in wild-type mice (Fig. 8 *B*). SFDR5 had no effect on neutrophil accumulation (data not shown). Blood was collected at the time of peritoneal lavage for total leukocyte count and differential which showed no significant difference between wild-type mice, Mac-1–deficient
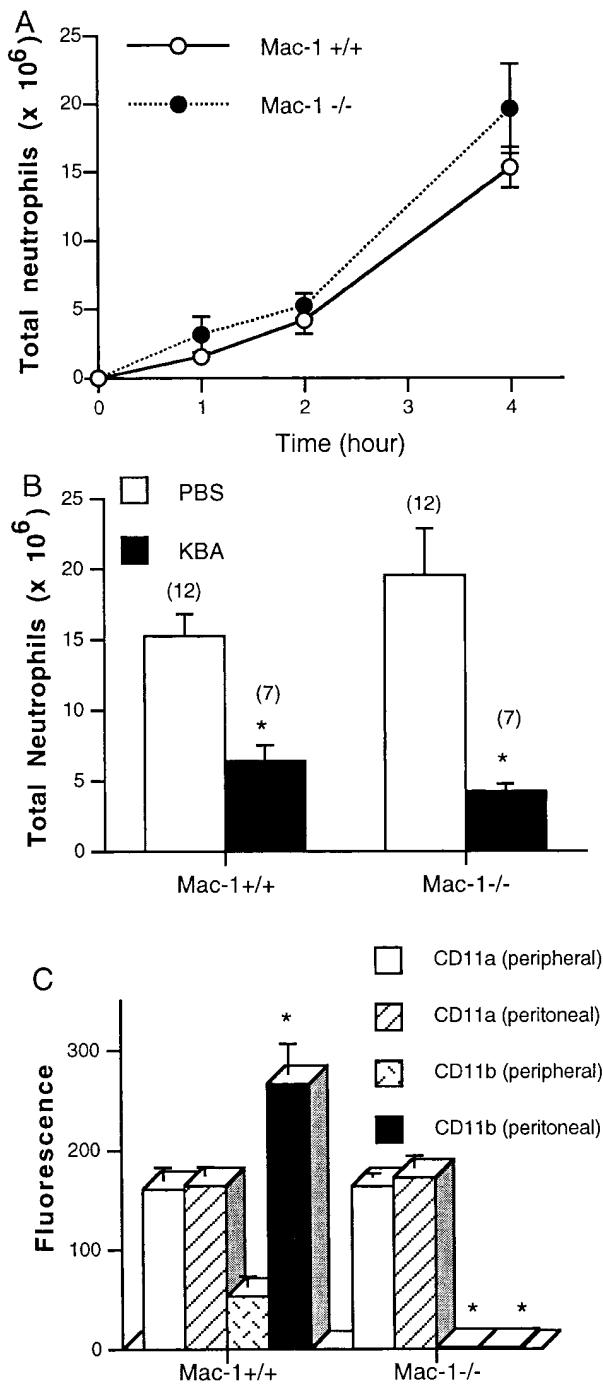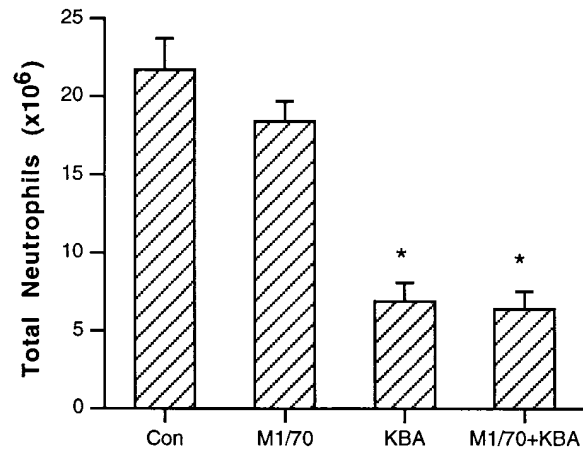
Figure 9. Effect of anti-CD11a and anti-CD11b on neutrophil influx in peritonitis. Wild-type mice were treated with PBS, anti-CD11a (KBA), anti-CD11b (M1/70), or the combination of anti-CD11a (KBA) and anti-CD11b (M1/70) intraperitoneally before thioglycollate injection. Peritoneal lavage was recovered 4 h after thioglycollate injection. Total neutrophil number = mean±SEM, $n = 6$, *$P < 0.05$.

mice $(-/-)$, and mice treated with mAbs (Table I). The increased percentage of neutrophils noted on the differential count is secondary to the intraperitoneal injection of thioglycollate. Neutrophil surface expression of CD11a remained the same after transmigration compared with that in peripheral blood. However, CD11b on neutrophils which had transmigrated into the peritoneal cavity was significantly upregulated in the wild-type mice compared with that on the peripheral neutrophils (Fig. 8 *C*). In additional experiments, the contribution of CD11b to neutrophil transmigration in wild-type mice was evaluated using F(ab′)₂ of M1/70 (anti-CD11b). This mAb reduced neutrophil accumulation by < 30%, which was not significant (Fig. 9). In contrast, KBA (anti-CD11a) reduced neutrophils numbers > 60% in these experiments (Fig. 9). Treatment with the combination of both M1/70 (anti-CD11b) and KBA (anti-CD11a) did not lead to further reduction of neutrophils than treatment with KBA alone (Fig. 9).

Assessment of neutrophil degranulation during peritonitis. Previous studies in humans have shown that neutrophils release granule contents at sites of acute inflammation, and studies in vitro indicate that adhesion enhances neutrophil secretory processes (22). We measured the β-glucuronidase content of peripheral and transmigrated neutrophils in the peritonitis model. 4 h after thioglycollate stimulation, the β-glucuronidase content in peritoneal neutrophils from wild-type mice was 35% of that in peripheral neutrophils (Fig. 10). In contrast, the β-glucuronidase content in peritoneal neutrophils from Mac-1–deficient mice remained 75% of that in peripheral neutrophils from these mice ($P < 0.05$ compared with wild-type mice, Fig. 10).

Figure 8. Kinetics of neutrophil influx in thioglycollate induced peritonitis. (*A*) Wild-type or CD11b-deficient mice as littermates were injected intraperitoneally with 1 ml of thioglycollate medium. At 1, 2, and 4 h after the injection, 3 ml of ice-cold PBS with 50 U/ml of heparin was injected intraperitoneally. Peritoneal lavage fluid was withdrawn and the total number of recovered neutrophils was determined. There is no significant difference between numbers of neutrophils recovered from the wild-type and the mutant mice at each time point. $n = 4$ (1 and 2 h), $n = 12$ (4 h). Values represent mean±SEM. (*B*) Effect of anti-CD11a on neutrophil influx in peritonitis. Wild-type CD11b-deficient mice as littermates were treated with 6 mg/kg anti-CD11a (KBA) intraperitoneally 16 h before and 9 mg/kg intravenously 1 h before thioglycollate injection. Peritoneal lavage was recovered 4 h after thioglycollate injection. Total neutrophil number = mean±SEM. Number of separate experiments indicated

above bars. *$P < 0.01$. (*C*) Surface expression of CD11a and CD11b of peripheral versus peritoneal neutrophils. Heparinized peripheral blood and peritoneal lavage leukocytes were incubated with FITC-labeled anti-CD11b (M1/70) or biotinylated KBA (anti-CD11a) for 15 min. Cells were fixed in 1% paraformaldehyde and collected on FACScan®. Values represent mean±SEM, $n = 12$, *$P < 0.001$.

Table I. Peripheral Blood Leukocyte Counts and Differential

			Differential (%)		
Genotype		Total WBC*	Neutrophil	Lymphs	Mono
		$\mu l \times 10^3$			
Mac-1+/+	$n = 7$	3.82±1.19	55±10.4	38.1±9.41	5.06±1.15
Mac-1−/−	$n = 7$	4.06±0.84	51.13±8.56	42.9±8.6	4.2±0.69
Mac-1+/+ (KBA)	$n = 9$	4.11±1.94	47.2±12.3	43.6±13.3	5.9±2.1
Mac-1−/− (KBA)	$n = 9$	3.39±0.76	60.1±10.4	31.5±10.4	4.27±0.65
Mac-1+/+ (SFDR5)	$n = 7$	4.12±1.44	54.8±9.85	36.2±9.4	4.94±0.81
Mac-1−/−(SFDR5)	$n = 7$	4.57±2.29	66.5±6.17	24.9±1.32	5.4±2.83
Mac-1+/+ (M1/70)	$n = 3$	6.16±1.71	42.7±16.57	47.7±17.5	4.87±1.91

*Peripheral white blood count ($\mu l \times 10^3$). Data expressed as mean±SEM. Percentage of polymorphonuclear leukocytes (neutrophils)/lymphocytes/monocytes from > 100 cells counted. Peripheral blood leukocyte counts were measured in all animals 4 h after intraperitoneal thioglycollate injection. Mac-1+/+ = wild-type mice. Mac-1−/− = homozygous Mac-1 mutants (KBA) = treatment with anti–LFA-1. (M1/70) = anti–Mac-1, (SFDR5) = isotype-matched control.

Assessment of Mac-1–dependent adhesion in vivo. Previous studies by Tang et al. (27) have shown that fibrinogen-coated PET disks implanted in the peritoneal cavity induce an acute inflammatory response with a resultant accumulation of leukocytes adherent to the implanted disks, a process that is almost completely abrogated by administration of the specific Mac-1 antagonist, recombinant neutrophil inhibitory factor. This model was used to assess Mac-1–dependent adhesion in the CD11b-deficient and wild-type mice. Peritoneal lavage collected 16 h after implanting the disks revealed that neutrophil emigration was not reduced in CD11b-deficient mice compared with wild-type mice (Fig. 11). In contrast, neutrophil ad-

hesion to fibrinogen-coated PET disks was markedly low in CD11b-deficient mice compared with normal mice ($P < 0.01$). Despite high levels of influx, neutrophils in the CD11b-deficient mice were unable to exhibit Mac-1–dependent adhesion.

Discussion

Patients who have a complete deficiency or extremely low levels of CD18 have severe defects in the inflammatory response with characteristic clinical features that include soft tissue lesions, impaired pus formation, defective wound healing, and
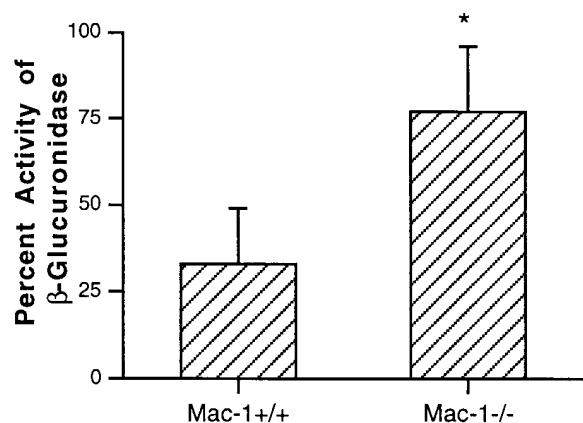

Figure 10. β-glucuronidase content of peritoneal exudate and peripheral neutrophils. Wild-type or CD11b-deficient mice as littermates were injected intraperitoneally with 1 ml of thioglycollate medium. 4 h after the injection, 3 ml of ice-cold PBS with 50 U/ml of heparin was injected intraperitoneally and peritoneal lavage fluid was withdrawn. After the total neutrophil number was determined from the blood and lavage fluid, the cell pellet was lysed in 0.2% Tween 20. An aliquot of 10^6 cells was added to 100 μl of 5 mg/ml phenolphthalein glucuronic acid, pH 4.6, and incubated at 37°C overnight. Reactions were stopped the second day by adding 1 ml of glycine (pH 10.2). Samples were then measured by spectrophotometer at 540 nm. Peritoneal neutrophil β-glucuronidase activity was divided by that of the peripheral as a total percentage of the enzyme retained after the transmigration. Values represent mean±SEM, $n = 4$, *$P < 0.05$.
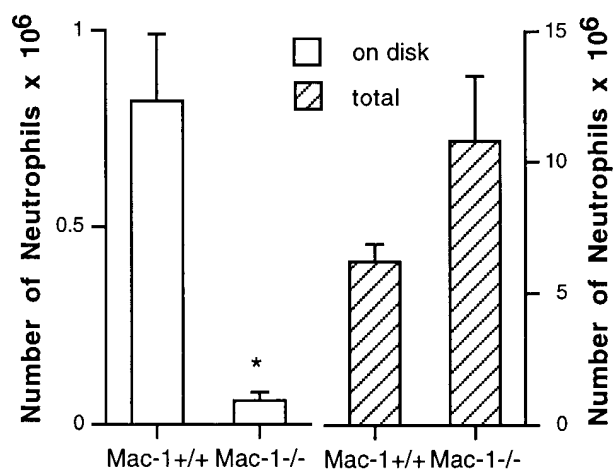

Figure 11. Neutrophil accumulation on the surface of fibrinogen-coated PET disks and in peritoneal lavage. Three disks were implanted intraperitoneally in each age-matched wild-type mouse and CD11b-deficient mouse. Peritoneal lavage using 5 ml warm PBS was performed 16 h later and PET disks were removed at the same time. Total cell count and differentials of the lavage were determined. MPO activity of the total cell pellet from the peritoneal lavage and cells adhered to the disks was determined. Empty bars represent neutrophils accumulated on fibrinogen-coated disks, hatched bars represent total neutrophil recruitment in the peritoneal cavity (disk plus lavage). Values represent mean±SEM, $n = 12$, *$P < 0.01$.

increased morbidity and mortality from bacterial infections. Targeted mutations of the murine *CD18* lead to a similar phenotype in the mouse as seen with LAD I. Mice with a complete deficiency of CD18 have an increased incidence of soft tissue infections, impaired growth, and increased morbidity and mortality from infections, whereas mice which express ∼ 10% of the normal level of CD18 have relatively normal growth and development (31, 32). To define the contributions of CD11b in vivo, we have developed mice deficient in CD11b by targeted homologous recombination in ES cells. Mice homozygous with a targeted mutation in *CD11b* were confirmed to have a null phenotype by flow cytometry, immunohistochemistry, and several in vitro assays for Mac-1 function. Mice with a complete deficiency of CD11b have normal growth and development as compared with wild-type littermates with a low incidence of infection (≈ 1%) when maintained in microisolator cages. In contrast, mice with a complete deficiency of CD18 when maintained under the same conditions exhibit a much higher incidence of poor growth and serious infection. Recently, mice with a complete deficiency of CD11a have also been developed and reported to have normal growth and development with a low incidence of infection (33). Thus, targeted mutations which lead to a complete deficiency of either CD11b or CD11a in the mouse do not reproduce the phenotype which is seen with a complete deficiency of CD18. The more severe phenotypic abnormalities exhibited by mutations in CD18 which result in a deficiency in all four of the CD18 integrins suggest that either CD11a/CD18 and CD11b/CD18 have some overlapping functions and both must be absent or that other members of the CD11/CD18 family such as CD11c and CD11d have important functions. Ongoing efforts to develop mice with a combined deficiency of CD11a and CD11b along with mutations in the other CD11 integrins should provide further insight.

Our results demonstrate that the rate of extravasation of neutrophils in the first 4 h of thioglycollate-induced peritonitis is not significantly abnormal in mice totally deficient in CD11b. Further confirmation that Mac-1 (CD11b/CD18) was unnecessary for neutrophil migration was provided by our observation that fibrinogen-coated PET disks in the peritoneal cavity had markedly fewer attached neutrophils in CD11b-deficient mice, even though there was as vigorous an influx of neutrophils as that seen in the normal animals. The neutrophils deficient in CD11b that migrated into the peritoneal cavity were defective in adhesion to fibrinogen-coated plastic disks, confirming that CD11b plays an essential role in the binding of neutrophils to fibrinogen (14, 27). Furthermore, this suggests that CD11c/CD18 is not markedly upregulated in these mice because CD11c/CD18 has also been shown to mediate neutrophil adhesion to fibrinogen-coated surfaces (34, 35). In addition, neutrophils from CD11b-deficient mice were also defective in neutrophil degranulation and iC3b-mediated phagocytosis. Future experiments should better define the importance in vivo of these functions of CD11b by using Mac-1–deficient mice in murine models of infection, inflammation, and healing. In contrast to the results which demonstrate that Mac-1 plays a critical function in mediating binding of leukocytes to fibrinogen, neutrophil degranulation, and iC3b-mediated phagocytosis, our results are inconsistent with the conclusion that CD11b/CD18 is necessary for effective emigration of neutrophils, an assumption based on earlier studies with anti-CD11b monoclonal antibodies 5C6 (7) and M1/70 (8) in similar models.

One possible explanation for the discrepancy between the studies using blocking antibodies and the CD11b-deficient mice was evident in the report by Rosen and Gordon (7). They found that 5C6 was inhibitory in the peritonitis model only when used as an IgG. The F(ab′)₂ preparation of this mAb was not significantly inhibitory. In the studies by Jutila et al. (8), M1/70 was also used as intact antibody where it produced ∼ 70% inhibition of peritoneal influx of neutrophils, but in this study, we found that F(ab′)₂ preparation of M1/70 was not significantly inhibitory in vivo, even though this preparation produced almost complete blocking of neutrophil adhesion to KLH-coated glass in vitro, a pattern like that produced by targeted deletion of CD11b. These observations suggest a possible secondary effect of the antibodies mediated through the Fc portion of the antibody molecule. We have observed that some intact antibodies activate neutrophils (22), which raises the concern that inhibitory effects of IgG M1/70 and 5C6 may be due in part to factors other than simple blocking of Mac-1–dependent adhesion.

In earlier studies, we (36) and others (37, 38) have found in an in vitro model of transendothelial migration that IL-1 stimulation of human umbilical vein endothelial cell monolayers resulted in a high level of transendothelial migration when previously unstimulated neutrophils contacted the monolayer. This migration was inhibited > 80% by anti-CD11a mAb alone, while anti-CD11b mAbs were ineffective. Similar results were obtained by Rutter et al. in a lapine model of dermal inflammation and peritonitis (12) and by Graf et al. in a lapine model of peritonitis (13). We have also found that in vitro chemotactic responses of neutrophils through human umbilical vein endothelial cell monolayers were more effectively inhibited by anti-CD11a mAbs than anti-CD11b (17). Issekutz et al. (11) observed that systemic administration of anti-CD11a mAb was more effective in reducing neutrophil localization than anti-CD11b in rat dermal inflammation induced by injection of ZAS (a source of C5a chemotactic factor), and Argenbright et al. (39) demonstrated in an intravital preparation of lapine mesenteric vessels superfused with C5a, that anti-CD11a and anti-CD18 mAbs induced equally marked inhibition of firm adhesion of leukocytes. Rosenbaum and Boney (40) reported similar observations in a rat model of uveitis. Thus, experimental observations in vivo in mice, rats, and rabbits reveal limited to absent contributions of Mac-1 to neutrophil emigration or transendothelial migration, and experimental results in vitro using human neutrophils and endothelial monolayers are congruent with these results. Development of mice deficient in CD11b and CD11a has provided an opportunity to study functions of the CD18 integrins which are potentially redundant without using mAbs. In contrast to the normal rate of neutrophil emigration in the first 4 h after thioglycollate-induced peritonitis in mice deficient in CD11b, emigration of neutrophils was reduced by ∼ 60% in mice deficient in CD11a (33), similar to the reductions achieved by antibodies to LFA-1 in wild-type mice in our experiments (Fig. 8 *B*). Neutrophil emigration in many inflammatory settings appears to be heavily dependent on LFA-1.

Though Mac-1 does not appear to be the dominant CD18 integrin in extravasation of neutrophils, it does play a cooperative or equivalent role with LFA-1 in some experiment conditions. For example, Nolte et al. (41) has shown that F(ab′)₂ preparations of mAb M1/70 inhibit leukocyte sticking in an intravital model of ischemia/reperfusion in murine dorsal skin

chambers. Similar intravital observations in rat and lapine models reveal similar contributions of Mac-1 to firm adhesion to venular endothelium (42, 43), and Issekutz et al. (11) found that after intradermal injection of IL-1 in rats, significant inhibition of neutrophil localization was obtained only with combined administration of anti-CD11b and anti-CD11b mAbs, suggesting that with that stimulus either Mac-1 or LFA-1 was sufficient for localization. Rote et al. (44) drew a similar conclusion from studies of reverse passive Arthus in rats. Our earlier studies using human and canine neutrophils and endothelial cells in vitro (16, 17, 45) revealed that complete inhibition of transendothelial migration was attained only when anti-CD11a and anti-CD11b mAbs were used in combination.

In contrast to the lesser role played in extravasation, experimental models (46–49) reveal Mac-1–dependent tissue injury. The possible functional significance of the differential use of Mac-1 and LFA-1 by neutrophils may be revealed in the following studies. It is now clear that Mac-1 (CD11b/CD18)-dependent adhesion greatly augments reactive oxygen release by neutrophils (22, 50), an event that is not inhibited by anti-CD11a mAbs. This also appears to be true for β-glucuronidase release during emigration into the peritoneal cavity as seen in our experiments with the CD11b-deficient mice. This adherence-dependent secretory activity occurs in vitro only after a lag phase of ∼ 60 min, a time far longer than the time for transendothelial migration. If transendothelial migration is principally dependent on LFA-1 (an integrin that appears not to signal the massive release of reactive oxygen [22]) and occurs rapidly, then the endothelial cell would likely be spared exposure to high concentrations of reactive oxygen. In contrast to the transient interaction with endothelium, studies have demonstrated that neutrophil adhesion to parenchymal cells expressing ICAM-1 may result in a cytotoxic effect that is blocked by anti-CD11b mAbs (45). These published studies and our experimental results in mice totally deficient in CD11b focus attention on an apparent dichotomy in the functions of neutrophil Mac-1 and LFA-1. LFA-1 seems to be more important in the process of emigration, while Mac-1 is more important in extravascular adhesive events that lead to tissue damage.

Acknowledgments

References

1. Anderson, D.C., F.C. Schmalstieg, S. Kohl, M.A. Arnaout, B.J. Hughes, M.F. Tosi, G.J. Buffone, B.R. Brinkley, W.D. Dickey, J.S. Abramson, et al. 1984. Abnormalities of polymorphonuclear leukocyte function associated with a heritable deficiency of high molecular weight surface glycoproteins (GP138). Common relationship to diminished cell adherence. *J. Clin. Invest.* 74:536–551.

2. Kishimoto, T.K., K. O'Connor, A. Lee, T.M. Roberts, and T.A. Springer. 1987. Cloning of the beta subunit of the leukocyte adhesion proteins: homology to an extracellular matrix receptor defines a novel supergene family. *Cell.* 48:681–690.

3. Corbi, A.L., T.K. Kishimoto, L.J. Miller, and T.A. Springer. 1988. The human leukocyte adhesion glycoprotein Mac-1 (complement receptor type 3, CD11b) alpha subunit: cloning, primary structure, and relation to the integrins, von Willebrand factor and factor B. *J. Biol. Chem.* 263:12403–12411.

4. Larson, R.S., A.L. Corbi, L. Berman, and T.A. Springer. 1989. Primary structure of the LFA-1 alpha subunit. An integrin with an embedded domain defining a protein superfamily. *J. Cell Biol.* 108:703–712.

5. Larson, R.S., and T.A. Springer. 1990. Structure and function of leukocyte integrins. *Immunol. Rev.* 114:181–217.

6. Van der Vieren, M., H. Le Trong, C.L. Wood, P.F. Moore, T. St. John, D.E. Staunton, and W.M. Gallatin. 1995. A novel leukointegrin, αdβ2, binds preferentially to ICAM-3. *Immunity.* 3:683–690.

7. Rosen, H., and S. Gordon. 1987. Monoclonal antibody to the murine type 3 complement receptor inhibits adhesion of myelomonocytic cells in vitro and inflammatory cell recruitment in vivo. *J. Exp. Med.* 166:1685–1701.

8. Jutila, M.A., L. Rott, E.L. Berg, and E.C. Butcher. 1989. Function and regulation of the neutrophil MEL-14 antigen in vivo: comparison with LFA-1 and MAC-1. *J. Immunol.* 143:3318–3324.

9. Jones, D.H., F.C. Schmalstieg, K. Dempsey, S.S. Krater, D.D. Nannen, C.W. Smith, and D.C. Anderson. 1990. Subcellular distribution and mobilization of Mac-1 (CD11b/CD18) in neonatal neutrophils. *Blood.* 75:488–498.

10. Hughes, B.J., J.C. Hollers, E. Crockett-Torabi, and C.W. Smith. 1992. Recruitment of CD11b/CD18 to the neutrophil surface and adherence-dependent cell locomotion. *J. Clin. Invest.* 90:1687–1696.

11. Issekutz, A.C., and T.B. Issekutz. 1992. The contribution of LFA-1 (CD11a)/CD18 and MAC-1 (CD11b/CD18) to the *in vivo* migration of polymorphonuclear leukocytes to inflammatory reactions in the rat. *Immunology.* 76:655–661.

12. Rutter, J., T.J. James, D. Howat, A. Shock, D. Andrew, P. De Baetselier, J. Blackford, J.M. Wilkinson, G. Higgs, B. Hughes, and M.K. Robinson. 1994. The *in vivo* and *in vitro* effects of antibodies against rabbit β2-integrins. *J. Immunol.* 153:3724–3733.

13. Graf, J.M., C.W. Smith, and M.M. Mariscalco. 1996. Contribution of LFA-1 and Mac-1 to CD18-dependent neutrophil emigration in a neonatal rabbit model. *J. Appl. Physiol.* 80:1984–1992.

14. Tang, L., and J.W. Eaton. 1993. Fibrin(ogen) mediates acute inflammatory response to biomaterials. *J. Exp. Med.* 178:2147–2156.

15. Muchowski, P.J., L. Zhang, E.R. Chang, H.R. Soule, E.F. Plow, and M. Moyle. 1994. Functional interaction between integrin antagonist neutrophil inhibitory factor and the I domain of CD11b/CD18. *J. Biol. Chem.* 269:26419–26423.

16. Smith, C.W., S.D. Marlin, R. Rothlein, C. Toman, and D.C. Anderson. 1989. Cooperative interactions of LFA-1 and Mac-1 with intercellular adhesion molecule-1 in facilitating adherence and transendothelial migration of human neutrophils in vitro. *J. Clin. Invest.* 83:2008–2017.

17. Furie, M.B., M.C.A. Tancinco, and C.W. Smith. 1991. Monoclonal antibodies to leukocyte integrins CD11a/CD18 and CD11b/CD18 or intercellular adhesion molecule-1 (ICAM-1) inhibit chemoattractant-stimulated neutrophil transendothelial migration *in vitro. Blood.* 78:2089–2097.

18. Pytela, R. 1988. Amino acid sequence of the murine Mac-1 alpha chain reveals homology with the integrin family and an additional domain related to von Willebrand factor. *EMBO (Eur. Mol. Biol. Organ.) J.* 7:1371–1378.

19. McMahon, A.P., and A. Bradley. 1990. The Wnt-1 (int-1) proto-oncogene is required for development of a large region of the mouse brain. *Cell.* 62:1073–1085.

20. Ramirez, S.R., P.J. Rivera, J.D. Wallace, M. Wims, H. Zheng, and A. Bradley. 1992. Genomic DNA microextraction: a method to screen numerous samples. *Anal. Biochem.* 201:331–335.

21. Truong, L.D., A. Farhood, J. Tasby, and D. Gillum. 1992. Experimental chronic renal ischemia: morphologic and immunologic studies. *Kidney Int.* 41:1676–1689.

22. Shappell, S.B., C. Toman, D.C. Anderson, A.A. Taylor, M.L. Entman, and C.W. Smith. 1990. Mac-1 (CD11b/CD18) mediates adherence-dependent hydrogen peroxide production by human and canine neutrophils. *J. Immunol.* 144:2702–2711.

23. Smith, C.W., J.C. Hollers, R.A. Patrick, and C. Hassett. 1979. Motility and adhesiveness in human neutrophils. Effects of chemotactic factors. *J. Clin. Invest.* 63:221–229.

24. Rochon, Y.P., M.M. Frojmovic, and E.L. Mills. 1990. Comparative studies of microscopically determined aggregation, degranulation, and light transmission after chemotactic activation of adult and newborn neutrophils. *Blood.* 75:2053–2060.

25. Anderson, D.C., M.L. Mace, B.R. Brinkley, R.R. Martin, and C.W. Smith. 1981. Recurrent infection in glycogenosis type 1b: abnormal neutrophil motility related to impaired redistribution of adhesion sites. *J. Infect. Dis.* 143:447–459.

26. Lee, H., and S. Rich. 1991. Co-stimulation of T cell proliferation by transforming growth factor-beta1. *J. Immunol.* 147:1127–1133.

27. Tang, L., T.P. Ugarova, E.F. Plow, and J.W. Eaton. 1996. Molecular determinants of acute inflammatory responses to biomaterials. *J. Clin. Invest.* 97:1329–1334.

28. Takeuchi, K., H. Wood, and R.T. Swank. 1986. Lysosomal elastase and cathepsin G in beige mice. Neutrophils of beige (Chediak-Higashi) mice selectively lack lysosomal elastase and cathepsin G. *J. Exp. Med.* 163:665–677.

29. Anderson, D.C., L.J. Miller, F.C. Schmalstieg, R. Rothlein, and T.A. Springer. 1986. Contributions of the Mac-1 glycoprotein family to adherence-dependent granulocyte functions: structure-function assessments employing subunit-specific monoclonal antibodies. *J. Immunol.* 137:15–27.

30. Sligh, J.E., Jr., C.M. Ballantyne, S.S. Rich, H.K. Hawkins, C.W. Smith, A. Bradley, and A.L. Beaudet. 1993. Inflammatory and immune responses are impaired in mice deficient in intercellular adhesion molecule 1. *Proc. Natl. Acad. Sci. USA.* 90:8529–8533.

31. Scharffetter-Kochanek, K., K. Norman, D.C. Bullard, I. Lorenzo, N.P. van Nood, H. Lu, S. Rich, W. Smith, K. Ley, and A.L. Beaudet. 1996. Generation and characterization of a CD18 complete knockout mouse: new insights in the function of the CD18 molecule. *J. Invest. Dermatol.* 106:809.

32. Wilson, R.W., C.M. Ballantyne, C.W. Smith, C. Montgomery, A. Bradley, W.E. O'Brien, and A.L. Beaudet. 1993. Gene targeting yields a CD18-mutant mouse for study of inflammation. *J. Immunol.* 151:1571–1578.

33. Schmits, R., T.M. Kundig, D.M. Baker, G. Shumaker, J.J.L. Simard, G. Duncan, A. Wakeham, A. Shahinian, A. van der Heiden, M.F. Bachmann, et al. 1996. LFA-1–deficient mice show normal CTL responses to virus but fail to reject immunogenic tumor. *J. Exp. Med.* 183:1415–1426.

34. Loike, J.D., B. Sodeik, L. Cao, S. Leucona, J.I. Weitz, P.A. Detmers, S.D. Wright, and S.C. Silverstein. 1991. CD11c/CD18 on neutrophils recognizes a domain at the N terminus of the Aα chain of fibrinogen. *Proc. Natl. Acad. Sci. USA.* 88:1044–1048.

35. Loike, J.D., R.L. Silverstein, S.D. Wright, J.I. Weitz, and S.C. Silverstein. 1992. The role of protected extracellular compartments in interactions between leukocytes, and platelets and fibrin/fibrinogen matrices. *Ann. NY. Acad. Sci.* 667:163–172.

36. Smith, C.W., R. Rothlein, B.J. Hughes, M.M. Mariscalco, F.C. Schmalstieg, and D.C. Anderson. 1988. Recognition of an endothelial determinant for CD18-dependent human neutrophil adherence and transendothelial migration. *J. Clin. Invest.* 82:1746–1756.

37. Moser, R., B. Schleiffenbaum, P. Groscurth, and J. Fehr. 1989. Interleukin 1 and tumor necrosis factor stimulate human vascular endothelial cells to promote transendothelial neutrophil passage. *J. Clin. Invest.* 83:444–455.

38. Kuijpers, T.W., B.C. Hakkert, M.H.L. Hart, and D. Roos. 1992. Neutrophil migration across monolayers of cytokine-prestimulated endothelial cells. A role for platelet-activating factor and IL-8. *J. Cell Biol.* 117:565–572.

39. Argenbright, L.W., L.G. Letts, and R. Rothlein. 1991. Monoclonal antibodies to the leukocyte membrane CD18 glycoprotein complex and to intercellular adhesion molecule-1 inhibit leukocyte-endothelial adhesion in rabbits. *J. Leukocyte Biol.* 49:253–257.

40. Rosenbaum, J.T., and R.S. Boney. 1993. Efficacy of antibodies to adhesion molecules, CD11a or CD18, in rabbit models of uveitis. *Curr. Eye Res.* 12:827–831.

41. Nolte, D., R. Hecht, P. Schmid, A. Botzlar, M.D. Menger, C. Neumueller, F. Sinowatz, D. Vestweber, and K. Messmer. 1994. Role of Mac-1 and ICAM-1 in ischemia-reperfusion injury in a microcirculation model of BALB/C mice. *Heart Circ. Physiol.* 36:H1320–H1328.

42. Kurose, I., D.C. Anderson, M. Miyasaka, T. Tamatani, J.C. Paulson, R.F. Todd III, J.R. Rusche, and D.N. Granger. 1994. Molecular determinants of reperfusion-induced leukocyte adhesion and vascular protein leakage. *Circ. Res.* 74:336–343.

43. Zimmerman, B.J., J.W. Holt, J.C. Paulson, D.C. Anderson, M. Miyasaka, T. Tamatani, R.F. Todd III, J.R. Rusche, and D.N. Granger. 1994. Molecular determinants of lipid mediator-induced leukocyte adherence and emigration in rat mesenteric venules. *Am. J. Physiol.* 266:H847–H853.

44. Rote, W.E., E. Dempsey, S. Maki, G.P. Vlasuk, and M. Moyle. 1996. The role of CD11/Cd18 integrins in the reverse passive arthus reaction in rat dermal tissue. *J. Leukocyte Biol.* 59:254–261.

45. Entman, M.L., K. Youker, T. Shoji, G.L. Kukielka, S.B. Shappell, A.A. Taylor, and C.W. Smith. 1992. Neutrophil induced oxidative injury of cardiac myocytes. A compartmented system requiring CD11b/CD18-ICAM-1 adherence. *J. Clin. Invest.* 90:1335–1345.

46. Argenbright, L.W., and R.W. Barton. 1993. Adhesion molecules in the shwartzman response. *In* Structure, Function and Regulation of Molecules Involved in Leukocyte Adhesion II. P.E. Lipsky, R. Rothlein, T.K. Kishimoto, R.B. Faanes, and C.W. Smith, editors. Springer-Verlag, New York. 306–313.

47. Jaeschke, H., A.I. Farhood, and C.W. Smith. 1991. Neutrophil-induced liver cell injury in endotoxin shock is a CD11b/CD18-dependent mechanism. *Am. J. Physiol.* 261:c1051–c1056.

48. Simpson, P.J., R.F. Todd III, J.C. Fantone, J.K. Mickelson, J.D. Griffin, and B.R. Lucchesi. 1988. Reduction of experimental canine myocardial reperfusion injury by a monoclonal antibody (anti-Mo1, anti-CD11b) that inhibits leukocyte adhesion. *J. Clin. Invest.* 81:624–629.

49. Chen, H., M. Chopp, R.L. Zhang, G. Bodzin, Q. Chen, J.R. Rusche, and R.F. Todd. 1994. Anti-CD11b monoclonal antibody reduces ischemic cell damage after transient focal cerebral ischemia in rat. *Ann. Neurol.* 35:458–463.

50. Nathan, C.F., S. Srimal, C. Farber, E. Sanchez, L. Kabbash, A. Asch, J. Gailit, and S.D. Wright. 1989. Cytokine-induced respiratory burst of human neutrophils. Dependence on extracellular matrix proteins and CD11/CD18 integrins. *J. Cell Biol.* 109:1341–1349.